Bioorganic & Medicinal Chemistry Letters 22 (2012) 7486–7489

Contents lists available at SciVerse ScienceDirect

Bioorganic & Medicinal Chemistry Letters

journal homepage: www.elsevier.com/locate/bmcl

Design and evaluation of azaindole-substituted *N*-hydroxypyridones as glyoxalase I inhibitors

Takashi Chiba, Jun Ohwada, Hiroshi Sakamoto, Takamitsu Kobayashi, Takaaki A. Fukami, Machiko Irie, Takaaki Miura, Kazuhiro Ohara, Hiroshi Koyano *

Research Division, Chugai Pharmaceutical Co., Ltd, 200 Kajiwara Kamakura, Kanagawa 247-8530, Japan

ARTICLE INFO

Article history:
Received 17 August 2012
Revised 3 October 2012
Accepted 9 October 2012
Available online 17 October 2012

Keywords:
Glyoxalase I (GLO1)
Structure-based drug design (SBDD)
N-Hydroxypyridone
7-Azaindole

ABSTRACT

We conducted a high throughput screening for glyoxalase I (GLO1) inhibitors and identified 4,6-diphenyl-*N*-hydroxypyridone as a lead compound. Using a binding model of the lead and public X-ray coordinates of GLO1 enzymes complexed with glutathione analogues, we designed 4-(7-azaindole)-substituted 6-phenyl-*N*-hydroxypyridones. 7-Azaindole's 7-nitrogen was expected to interact with a water network, resulting in an interaction with the protein. We validated this inhibitor design by comparing its structure-activity relationship (SAR) with that of corresponding indole derivatives, by analyzing the binding mode with X-ray crystallography and by evaluating its thermodynamic binding parameters.

Glyoxalase I (GLO1) is a zinc enzyme that catalyzes the isomerization of a hemithioacetal, formed from glutathione (GSH) and methylglyoxal (MG), to lactic acid thioester. The potential of GLO1 as a drug target for cancer and other diseases has been discussed over the last several decades.[1] GSH analogues,[2] flavonoids,[3] curcumins,[4] and a benzothiazole derivative[5] are reported to show moderate to potent GLO1 inhibitory activity and are expected to be evaluated further for practical uses.

We conducted a discovery program of non-peptidic GLO1 inhibitors through lead generation from high throughput screening (HTS) followed by rational inhibitor design using human GLO1/GSH analogue cocrystal structural data deposited in Protein Data Bank (PDB).[6–8] We analyzed the ligand–protein interactions observed in those structures and found that the following interactions are commonly observed: (1) hydrophobic interactions of ligands' substituents on the sulfur atom in a hydrophobic pocket; (2) a hydrogen bond between cysteine NH of ligands and a water molecule (hereafter referred to as W1) bound to Thr101A and Glu99A; (3) CH/π interaction between alkyl chain of γ-glutamic acid of ligands and Phe67A of the protein; (4) ionic interactions between the γ-glutamyl carboxylate/ammonium groups of ligands and Arg37A/Asn103A/Arg122B of the protein (Fig. 1).[9]

We conducted an HTS and identified a few hundred compounds whose GLO1 IC_{50} values were less than 10 μM. The majority of them had apparent zinc binding functional groups, which was anticipated from the nature of the GLO1 catalytic site. Among them, 4,6-diphenyl-*N*-hydroxypyridone (**1**) was found to have more potent GLO1 inhibitory activity (IC_{50} = 1.2 μM) than a well-known GLO1 inhibitor, *S*-(*p*-bromobenzyl)glutathione (*p*BBG)[2a] (IC_{50} = 21 μM, in-house data),[11] as well as good stability in serum and against liver microsomal oxidation (Fig. 2).

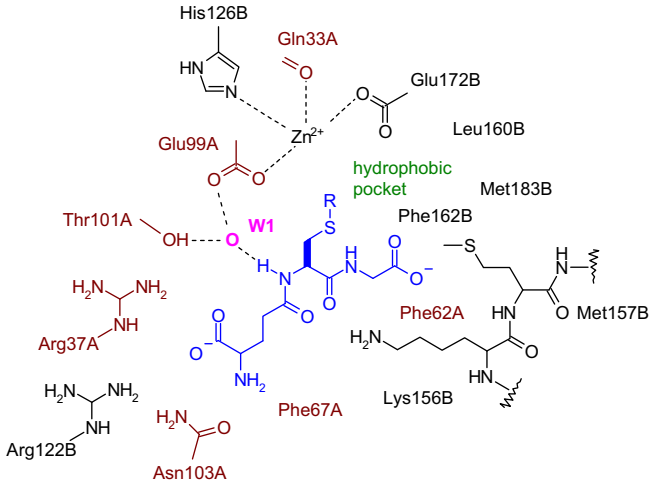

Figure 1. Schematic drawing of the interactions found in X-ray cocrystal structures of GLO1 and GSH analogs (R group, PDB code): R = benzyl, 1FRO;[6] R = *n*-hexyl, 1BH5;[7] R = 4-I-Ph-N(OH)C(O)–, 1QIN;[8] R = 4-NO_2–BnOC(O)–, 1QIP.[8] GLO1 catalytic site is composed of two peptide chains (A and B).[10]

* Corresponding author.
E-mail address: koyanohrs@chugai-pharm.co.jp (H. Koyano).

0960-894X/$ - see front matter © 2012 Elsevier Ltd. All rights reserved.
http://dx.doi.org/10.1016/j.bmcl.2012.10.045

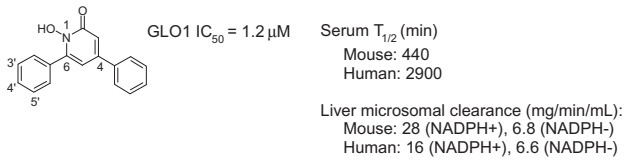

Figure 2. Structure and property of 4,6-diphenyl-*N*-hydroxypyridone (**1**).

A binding model of compound **1** was generated by its docking into the GLO1 catalytic site of a complex with zinc-coordinating *S*-(*N*-hydroxy-*N*-(*p*-iodophenyl)carbamoyl)glutathione (PDB code:1QIN)[8] in which the position of the two zinc-coordinating oxygen atoms was maintained. The probable binding mode is depicted in Figure 3. Another mode of zinc-coordination with alternative positions for N–O and C=O was denied because of severe steric repulsion between two phenyl groups and protein. In the model, 4-phenyl group of **1** was situated in the hydrophobic pocket (composed of Phe62A, Cys60A, Ile88A, Leu92A, Met157B, Met179B, Leu182B and Met183B) making an edge-to-face aromatic interaction with Phe62A. 6-Phenyl group of **1** was situated at the space which γ-glutamyl moiety of GSH analogues occupied (GSH binding pocket). Phe162B made an edge-to-face interaction with the 6-phenyl ring. No steric repulsion of **1** with W1 was observed (Fig. 3).

Since the zinc-coordination of *N*-hydroxypyridone fixed the vector of 4- and 6-substituents, we thought structure-activity relationship (SAR) of each substituent is independent and the combination of each optimized substituent would results in the best optimized compound. The first step of our lead optimization was to find alternative groups for the 4-phenyl group of **1** to enhance hydrophobic interaction in the hydrophobic pocket while still keeping the 6-phenyl group. Creighton et al. reported a positive correlation between competitive inhibition constant (K_i) and the Hansch hydrophobicity constant of aryl and alkyl group of *S*-(*N*-hydroxy-*N*-aryl/alkylcarbamoyl)glutathiones.[13] Therefore we prepared several 6-phenyl *N*-hydroxypyridones bearing a hydrophobic substituent at 4-position. Among them (**1**, **2a–2f**), **1** was the most potent. 3-Thienyl (**2a**), a bioisostere of the phenyl group, kept its activity but 3-pyridinyl (**2b**) decreased in activity, presumably because of its hydrophilicity. 4-Substituted phenyl groups (**2c** and **2d**) also decreased activity indicating limited space around the 4-position of the phenyl group. Non-aromatic substituents, 1-butynyl and butyl group (**2e** and **2f**, respectively) lost activity. This result indicates that the edge-to-face aromatic interaction between the phenyl group and Phe62A is important (Table 1). Accordingly, we kept the phenyl group at 4-position during the following modifications.

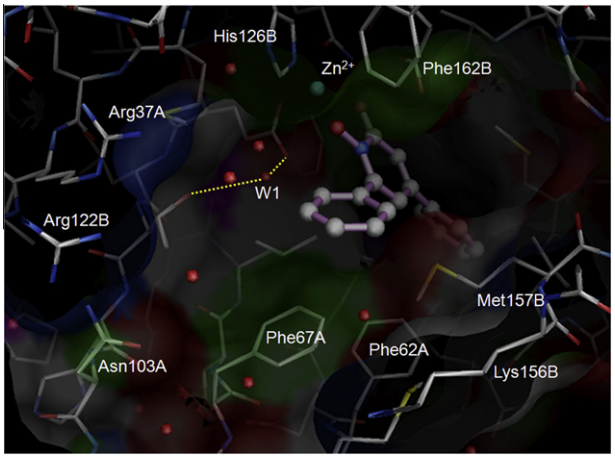

Figure 3. Binding model of **1**. The model was created using MOLOC.[12] Color surface is shown in green (hydrophobic), blue (donor), red (acceptor) and purple (hydrophilic).

Table 1
GLO1 inhibitory activity of 6-phenyl-*N*-hydroxypyridones with various substituents at 4-position

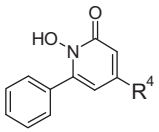

Compound	R^4	GLO1 IC_{50} (μM)
1		1.19
2a		1.52
2b		8.28
2c	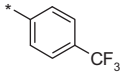	8.13
2d	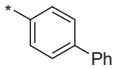	8.40
2e	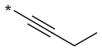	>10
2f	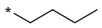	>10

Next, we designed substituents of the 6-position. Edge-to-face aromatic interaction between aromatic ring of ligand and Phe162B needed to be retained because the interaction seems to be important for tight binding. 3′-Position of the 6-phenyl group of **1** directs to a hydrophilic space where W1 exists. On the other hand, 4′-and 5′-positions of the 6-phenyl ring directs to a hydrophobic pocket surrounded by side-chains of residues Lys156B, Met157B and Phe162B. From these observations, we designed 7-azaindole whose 7-nitrogen faces the hydrophilic space and 5-membered ring occupies the hydrophobic pocket. The substituent on 1 N-position, which directs to the solvent-accessible region and therefore may contribute to the solubility of inhibitors, should be explored. To understand the function of 7-azaindole, we prepared the corresponding indole derivatives and evaluated them in parallel.

We did not employ the ionic interactions with Arg37A/Asn103A/Arg122B in our inhibitor design because introducing a carboxylate and/or an ammonium functional group to the *N*-hydroxypyridone scaffold would result in inhibitors with poor cell permeability.

The SAR of azaindole derivatives is shown in Table 2 along with the corresponding indole derivatives. 1 N-unsubstituted 7-azaindole (**3a**) and indole (**4a**) equally showed better activity than **1**. 3-Carbamoyl-benzyl (**3b**) and methoxyalkyl groups (**3c** and **3d**) on 1 N-position of 7-azaindole showed significant improvement in activity but the same substituents on indole (**4b–4d**) did not show such an effect.

We solved a cocrystal structure of **3d**/GLO1 complex at a resolution of 1.5 Å (Fig. 4, PDB code:3VW9). An asymmetric unit contains two active sites located at the interface of two peptide chains (A and B). The structure revealed that *N*-hydroxypyridone of compound **3d** coordinated a zinc cation (d(NO···Zn) = 2.4 Å, d(CO···Zn) = 2.2 Å). 4-Phenyl group, which made the edge-to-face interaction with Phe62A (d(Phe62A···4-Ph π face) = 4.3 Å), was

Table 2
GLO1 inhibitory activity of 4-phenyl-*N*-hydroxypyridones bearing 7-azaindole or indole moiety at 6-position

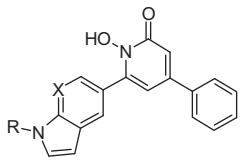

Compound	X	R	GLO1 IC_{50} (μM)
3a	N	H–	0.28
4a	CH		0.25
3b	N	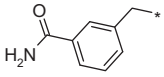	0.040
4b	CH		0.48
3c	N	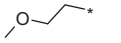	0.014
4c	CH		0.26
3d	N	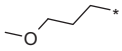	0.011
4d	CH		0.30

situated in the hydrophobic pocket. Azaindole was situated at the GSH binding pocket, forming an edge-to-face interaction with Phe162B (d(Phe162B···7-azaindole π face) = 4.0 Å). Phe67A was near 7-azaindole π face (d(Phe67A···7-azaindole π face) = 4.5 Å). Azaindole pyridine nitrogen made a hydrogen bond with a water (d(N···O) = 2.8 Å) in the hydrogen bond network including W1. A methoxypropyl group directed to Phe162B (d(Phe162B···-***C***H_2OMe) = 3.9 Å) and Trp170B (d(Trp170B···***C***H_2OMe) = 3.5 Å). Oxygen in the alkyl chain reached the solvent-accessible region.

Thermodynamic parameters of inhibitor binding (**3d** and **4d**) to GLO1 were determined by isothermal titration calorimetry (Fig. 5). As expected from the hydrogen bond network including azaindole observed in the X-ray structure, the binding of **3d** was enthalpic driven ($\Delta H = -11.1 \pm 1.2$ kcal/mol, $-T\Delta S = 2.1 \pm 1.0$ kcal/mol). Such enthalpy-driven binding was not observed for indole **4d** ($\Delta H = -6.3 \pm 1.7$ kcal/mol, $-T\Delta S = -2.0 \pm 1.4$ kcal/mol). Since the 1 N-unsubstituted derivatives **3a** and **4a** did not show a difference in activity, the stabilization of the water network is affected by substituents at this position. The dependence of hydrogen bond strengths on microenvironment polarity is reported in stabilization of protein structure.[14] We assume that the stabilization of the water network was achieved by **3d**, and resulted in improved activity.

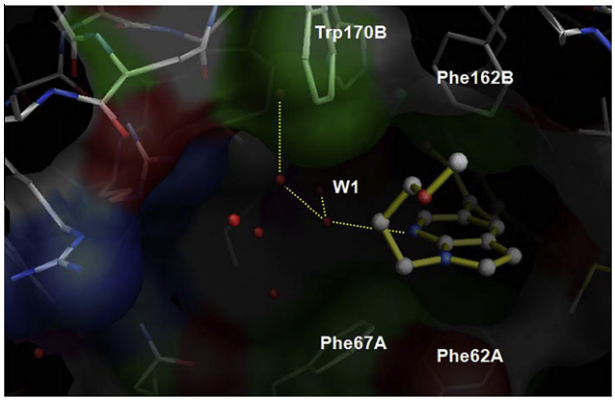

Figure 4. X-ray cocrystal structure of **3d**/GLO1 (PDB ID:3VW9).

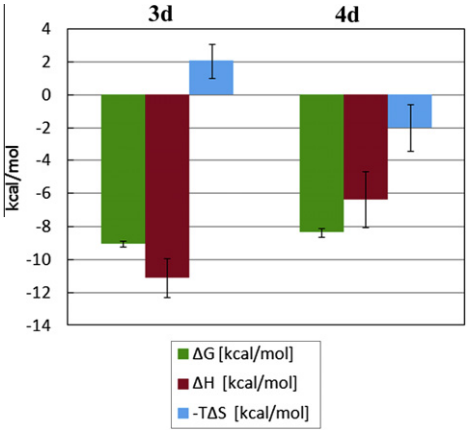

Figure 5. Thermodynamic parameters of **3d** and its indole counterpart **4d.**

The effect of oxygen in the 1 N-substituent was investigated by the comparison with carbon analogues (Table 3). Simple alkyl groups (**3e** and **3f**) were not effective in enhancing activity. Since oxygen in the alkyl chain of **3d** stayed in the solvent-accessible region, simple alkyl groups were unfavorable in such a hydrophilic environment.

Preparation of **3d** was performed starting from 2,6-dichloropyridineoxide (**5**) via iridium-catalyzed bolyration,[15] Suzuki coupling, de-chlorinating hydrolysis, and methoxymethyl (MOM) protection to give an intermediate **8**. Suzuki coupling of **8** with boronate **9** followed by alkylation at 1 N-position under basic conditions and subsequent deprotection afforded **3d** (Scheme 1).[16]

In summary, we discovered 7-azaindole substituted *N*-hydroxypyridone **3d** as a potent zinc-binding GLO1 inhibitor (IC_{50} = 11 nM) through lead generation from HTS and structure-based inhibitor design. The X-ray cocrystal structure and the comparison of binding energies with the indole counterpart **4d** revealed that **3d** bound to the water network and its binding was enthalpy-driven. Methoxypropyl chain of **3d** is essential for potent activity and this chain seems to stabilize the water network by strengthening neighboring hydrogen bonds. Other approaches of lead optimization for new GLO1 inhibitors will be discussed in future publications.

Table 3
The effect of oxygen on alkyl chain

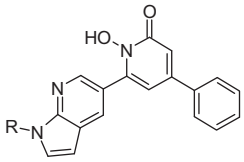

Compound	R	GLO1 IC_{50} (μM)
3c	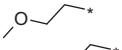	0.014
3d	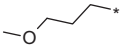	0.011
3e	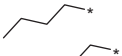	0.30
3f	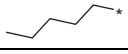	0.51

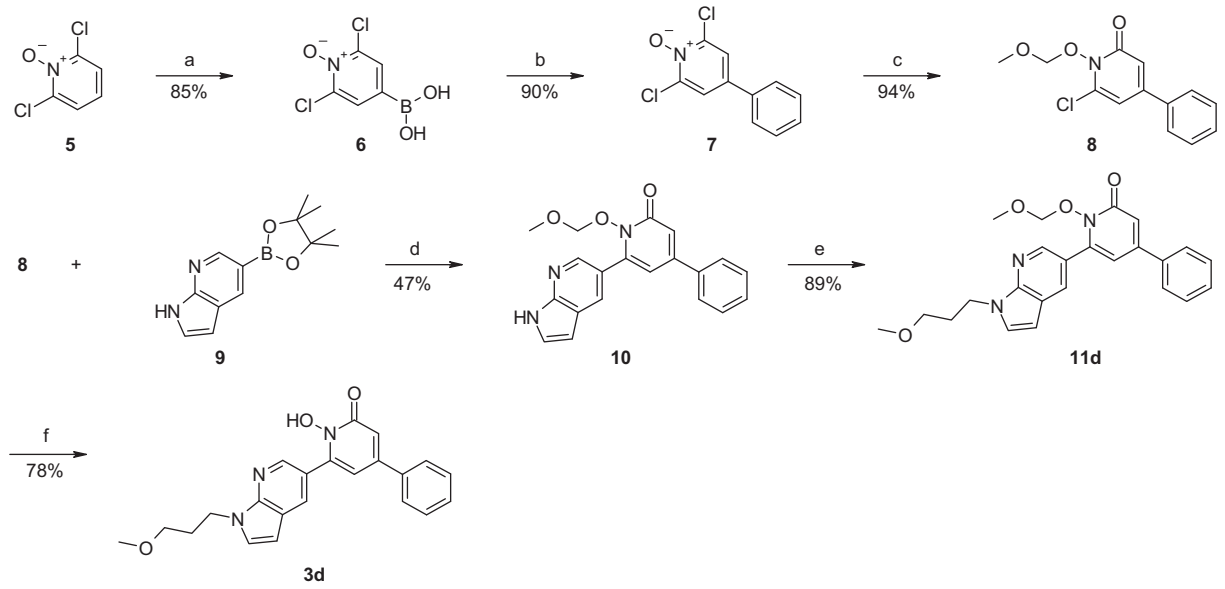

Scheme 1. Preparation of **3d**.[a] [a]Reagents and conditions: (a) $[Ir(OMe)COD]_2$, dtbpy, bis(pinacolato)diboron; (b) $PdCl_2(PPh_3)_2$, iodobenzene, Na_2CO_3 aq, NMP; (c) (i) 1 M NaOH aq, DMSO, 70 °C; (ii) MOMCl, DIPEA, CH_2Cl_2, rt; (d) $PdCl_2(PPh_3)_2$, Na_2CO_3 aq, NMP, 70 °C; (e) $MeO(CH_2)_3Cl$, 5 M NaOH aq, DMF; (f) 4 M HCl/AcOEt, ethyleneglycol, THF.

Acknowledgments

We thank Yasushi Sakaguchi, DKSH Japan K.K., for his help in conducting ITC measurements.

Supplementary data

Supplementary data associated with this article can be found, in the online version, at http://dx.doi.org/10.1016/j.bmcl.2012.10.045.

References and notes

1. Cell biology of glyoxalase in microbial systems and human disease: Thornalley, P. J.; Rabbani, N. *Semin. Cell Dev. Biol.* **2011**, *22*, 261.
2. (a) Vince, R.; Daluge, S. *J. Med. Chem.* **1971**, *14*, 35; (b) More, S. S.; Vince, R. *J. Med. Chem.* **2009**, *52*, 4650; (c) Al-Timari, A.; Douglas, K. T. *Biochim. Biophys. Acta* **1986**, *870*, 160; (d) Lo, T. W.; Thornalley, P. J. *Biochem. Pharmacol.* **1992**, *44*, 2357; (e) Hamilton, D. S.; Creighton, D. J. *J. Biol. Chem.* **1992**, *267*, 24933; (f) Murthy, N. S.; Bakeris, T.; Kavarana, M. J.; Hamilton, D. S.; Lan, Y.; Creighton, D. J. *J. Med. Chem.* **1994**, *37*, 2161.
3. Takasawa, R.; Takahashi, S.; Saeki, K.; Sunaga, S.; Yoshimori, A.; Tanuma, S. *Bioorg. Med. Chem.* **2008**, *16*, 3969.
4. Santel, T.; Pflug, G.; Hemda, N. Y. A.; Schäfer, A.; Hollenbach, M.; Buchold, M.; Hintersdorf, A.; Lindner, I.; Otto, A.; Bigl, M.; Oerlecke, I.; Hutschenreuter, A.; Sack, U.; Huse, K.; Groth, M.; Birkemeyer, C.; Schellenberger, W.; Gebhardt, R.; Platzer, M.; Weiss, T.; Vijayalakshmi, M. A.; Krüger, M.; Birkenmeier, G. *PLoS One* **2008**, *3*, e3508.
5. Takasawa, R.; Tao, A.; Saeki, K.; Shionozaki, N.; Tanaka, R.; Uchiro, H.; Takahashi, S.; Yoshimori, A.; Tanuma, S. *Bioorg. Med. Chem. Lett.* **2011**, *21*, 4337.
6. Cameron, A. D.; Olin, B.; Ridderström, M.; Mannervik, B.; Jones, T. A. *EMBO J.* **1997**, *16*, 3386.
7. Ridderström, M.; Cameron, A. D.; Jones, T. A.; Mannervik, B. *J. Biol. Chem.* **1998**, *273*, 21623.
8. Cameron, A. D.; Ridderström, M.; Olin, B.; Kavarana, M. J.; Creighton, D. J.; Mannervik, B. *Biochem.* **1999**, *38*, 13480.
9. For a detained discussion of non-covalent interactions, see: Bissantz, C.; Kuhn, B.; Starhl, M. *J. Med. Chem.* **2010**, *53*, 5061.
10. He, M. M.; Clugston, S. L.; Honek, J. F.; Matthews, B. W. *Biochemistry* **2000**, *39*, 8719.
11. GLO1 inhibitory activity was evaluated by examining the decrease in reduced glutathione (GSH). Recombinant human GLO1 protein is expressed in *Escherichia coli* BL21-CodonPlus. The test compound was incubated with sodium phosphate (50 mM, pH 7.0) containing $MgCl_2$ (12 mM), reduced GSH (0.1 mM), methylglyoxale (0.5 mM), and purified human GLO1 protein (8.75 ng) for 1 h at 37 °C. 5,5′-Dithiobis(2-nitrobenzoic acid) (Ellman's reagent) (0.67 mM) in sodium phosphate (10 mM, pH 7.0) was added at room temperature. After 10 min, the absorbance was measured at 450 nm.
12. Gerber, P. R.; Müller, K. *J. Comput. Aided Mol. Des.* **1995**, *9*, 251.
13. Kalsi, A.; Kavarana, M. J.; Lu, T.; Whalen, D. L.; Hamilton, D. S.; Creighton, D. J. *J. Med. Chem.* **2000**, *43*, 3981.
14. Gao, J.; Bosco, D. A.; Powers, E. T.; Kelly, J. W. *Nat. Struct. Mol. Biol.* **2009**, *16*, 684.
15. Ishiyama, T.; Miyaura, N. *Pure Appl. Chem.* **2006**, *78*, 1369.
16. Spectral data of **3d**: ^1H NMR (400 MHz, DMSO-d_6) δ: 11.51 (br s, 1H), 8.55 (d, J = 1.99 Hz, 1H), 8.30 (d, J = 1.99 Hz, 1H), 7.8 (m, 2H), 7.65 (d, J = 3.52 Hz, 1H), 7.40-7.54 (m, 3H), 6.85 (d, J = 2.63 Hz, 1H), 6.58 (d, J = 2.63 Hz, 1H), 6.56 (d, J = 3.52 Hz, 1H), 4.28 (t, J = 7.05 Hz, 2H), 3.32 (t, J = 6.17 Hz, 2H), 3.24 (s, 3 H), 2.06 (tt, J = 6.17, 7.05 Hz, 2H). MS (ESI^+) 376 $[M+H]^+$.